

## Highlights

- Granulometric fractionation (GF) and GF + micronization (GFM) reduce particle size
- GF and GFM increase olive pomace (OP) phenolic compounds (PC) that reach colon
- Tyrosol (tyr) and hydroxy-tyr (OH-tyr) were the major PC in colonic fermentation
- GFM released more tyr and OH-tyr from OP during colonic fermentation
- Only GFM-modified OP samples had oleuropein in the colonic phase of digestion

This work is licensed under CC BY-NC-ND 4.0

1     **Effect of micronization on olive pomace biotransformation in the static model of**  
2                                    **colonic fermentation**

3

4     Camila Sant'Anna Monteiro <sup>a,b</sup>, Paula Colpo Bortolazzo <sup>b</sup>, Camila Araujo Amorim Bonini  
5     <sup>b</sup>, Luana Tamires Dluzniewski <sup>b</sup>, Dariane Trivisiol da Silva <sup>b</sup>, Julia Baranzelli <sup>a,b</sup>, Franciele  
6     Aline Smaniotto <sup>a,b</sup>, Cristiano Augusto Ballus <sup>a</sup>, Jesús Lozano-Sánchez <sup>c</sup>, Sabrina Somacal  
7     <sup>a,b</sup>, Tatiana Emanuelli <sup>a,b</sup>

8

9     <sup>a</sup> Graduate Program on Food Science and Technology, Center of Rural Sciences, Federal  
10     University of Santa Maria, 97105-900, Santa Maria, RS, Brazil

11     <sup>b</sup> Integrated Center for Laboratory Analysis Development (NIDAL), Department of Food  
12     Technology and Science, Center of Rural Sciences, Federal University of Santa Maria,  
13     97105-900, Santa Maria, RS, Brazil

14     <sup>c</sup> Research and Development of Functional Food Centre (CIDAF), Bioregion building,  
15     PTS Granada, Avda. del Conocimiento 37, 18016 Granada, Spain.

16

17     \***Corresponding author.** Integrated Center for Laboratory Analysis Development  
18     (NIDAL), Department of Food Technology and Science, Center of Rural Sciences,  
19     Federal University of Santa Maria, 97105-900, Santa Maria, RS, Brazil; Tel.: +55 55 3220  
20     8547; fax: +55 55 3220 8353. E-mail address: [tatiana.emanuelli@ufsm.br](mailto:tatiana.emanuelli@ufsm.br) (Tatiana  
21     Emanuelli).

22

23     **Abbreviations:** Abbreviations: GF, granulometrically fractionated OP; GFM,  
24     granulometrically fractionated and micronized OP; IN: fraction that remains inside the  
25     dialysis tube and corresponds to the digesta that will reach the colon; IN-GF, IN-OP from

26 granulometrically fractionated OP; IN-GFM, IN-OP from granulometrically fractionated  
27 and micronized OP; IN-NF, IN-OP from non-fractionated OP; IN-OP: olive pomace  
28 fraction that was not bioaccessible after gastrointestinal digestion; NF, non-fractionated  
29 OP; OP, olive pomace; OUT, fraction that crosses the dialysis membrane and represents  
30 the bioaccessible fraction; UHPLC-MS/MS, ultra high-performance liquid  
31 chromatograph coupled to a triple-quadrupole mass spectrometer.

32

### 33 **Abstract**

34 The effect of granulometric fractionation and micronization of olive pomace (OP) on the  
35 biotransformation of phenolic compounds by intestinal microbiota was investigated *in*  
36 *vitro*. Three types of powdered OP samples were incubated with human feces to simulate  
37 colonic fermentation, after a sequential static digestion: non-fractionated OP (NF),  
38 granulometrically fractionated OP (GF) and granulometrically fractionated and  
39 micronized OP (GFM). GF and GFM favored the release of hydroxytyrosol, oleuropein  
40 aglycone, apigenin and phenolic acid metabolites in the first hours of colonic fermentation  
41 compared to NF (up to 41-fold higher). GFM caused higher release of hydroxytyrosol  
42 than GF. GFM was the only sample to release tyrosol and sustained tyrosol levels up to  
43 24 h of fermentation. Micronization associated with granulometric fractionation was  
44 more efficient than granulometric fractionation alone to increase the release of phenolic  
45 compounds from the OP matrix during simulated colonic fermentation and can be further  
46 studied for nutraceutical purposes.

47 **Keywords:** phenolic compounds, *in vitro* digestion, gut phenolic metabolites, superfine  
48 grinding

49

## 50 **1. Introduction**

51           The extraction of olive oil generates olive pomace (OP) that contains pulp, peel  
52 and stones and amounts to 80% of the processed fruits. Due to its chemical characteristics  
53 and the great volume produced, OP stands out for its potential to pollute the environment.  
54 OP is rich in vitamins, residual lipids, and dietary fiber, but the high content of insoluble  
55 fiber such as lignin prevents its direct use in food (Dermeche et al., 2013; Speroni et al.,  
56 2019). Additionally, this residue contains significant amounts of phenolic compounds,  
57 about 95-96% of the phenolic compounds present in the olive remain in the residue after  
58 the extraction of olive oil (Rodríguez-López et al., 2020). Generally, the residue is  
59 destined for energy production or as a soil fertilizer, however, studies show that OP can  
60 be an interesting source of bioactive compounds for food application (Rocchetti et al.,  
61 2020).

62           Processes that modify the fibrous matrix and increase its functionality can be  
63 useful for adding value to agri-food by-products as demonstrated by Speroni et al. (2020)  
64 for the micronization of OP. This ultrafine milling method reduces particle size to less  
65 than 100 µm and improves food dispersibility. Furthermore, the increased solubility of  
66 nutritive components would likely improve their intestinal absorption (Chen et al., 2018;  
67 Shu et al., 2019). Our research group has recently demonstrated that short time  
68 micronization of OP (less than 30 min) is efficient to increase the extractability of  
69 phenolic compounds and antioxidant capacity (Speroni et al., 2019). In addition, long-  
70 time micronization of OP (5 h) has been shown to be efficient for reducing lignin content  
71 and increasing soluble fiber content (Speroni et al., 2020). Long-time micronization of  
72 OP has been also shown to increase the release of phenolic compounds in the salivary and  
73 gastric phases during simulated *in vitro* static digestion, resulting in increased antioxidant  
74 capacity (Speroni et al., 2021). Moreover, long-time micronization of OP has been shown

75 to increase the intestinal bioaccessibility of hydroxytyrosol, decarboxymethyl oleuropein  
76 aglycone, oleuropein, luteolin, and apigenin in a static digestion model. Thus,  
77 micronization can be potentially used for the transformation and reuse of food by-  
78 products by increasing the bioaccessibility of bioactive compounds, the soluble dietary  
79 fiber content and powder functional properties (Zhao et al., 2018; Li et al., 2022). An  
80 avenue of possibilities will be opened for industrial application of micronization, which  
81 is already used (through ball milling) in the food and pharmaceutical industries to improve  
82 the dispersibility of different powder ingredients/components (Shu et al., 2019; Dhiman  
83 & Prabhakar, 2021).

84 Phenolic compounds of OP are mostly composed by phenolic alcohols  
85 (hydroxytyrosol and tyrosol), secoiridoids (oleuropein and its derivatives), flavonoids  
86 (luteolin), and phenolic acids (caffeic acid and *p*-coumaric acid) (Malapert et al., 2018).  
87 These compounds have been described to reduce the risk of cardiovascular diseases and  
88 some types of cancer, by exerting an antioxidant effect, neutralizing reactive species and  
89 oxidative reactions (Conterno et al., 2019; Covas et al., 2006; Serreli & Deiana, 2018).  
90 However, a small fraction of phenolic compounds is absorbed intact up to the small  
91 intestine and can exert their systemic effects in the native form (Augusti et al., 2021).  
92 According to Rocchetti et al. (2020), the bioaccessibility of phenolic acids and  
93 secoiridoids in olive oil was low during digestion (10-25%), whereas phenolic alcohols,  
94 mainly hydroxytyrosol, was the only one that showed higher bioaccessibility (> 60%).  
95 Compounds with a complex structure resist to the acidic conditions of stomach and will  
96 be found at significant amounts in the non-absorbable fraction in the small intestine  
97 (Mosele et al., 2015). After reaching the colon, they become available for metabolism by  
98 intestinal microbiota (Rodríguez-López et al., 2020; Gil-Sánchez et al., 2018). The  
99 products formed during the biotransformation of phenolic compounds have low

100 molecular weight, resulting in greater availability for absorption and in some cases greater  
101 biological activity than their parent compounds (Augusti et al., 2021). In addition,  
102 phenolic compounds that reach the large intestine can reshape the intestinal microbiota  
103 exerting a prebiotic-like effect (Augusti et al., 2021; Ribeiro et al., 2021).

104         Studies on the biotransformation that micronized OP suffers during digestion and  
105 colonic fermentation can provide information about the bioaccessibility of phenolic  
106 compounds in the small intestine and the microbial-derived phenolic metabolites that are  
107 likely implicated in the bioactive properties of dietary phenolic compounds. The  
108 hypothesis of the study is that micronization of OP enhances the amount of phenolic  
109 compounds released during colonic fermentation by increasing the solubility of the food  
110 matrix and their interaction with gut microbiota. Thus, the objective of this study was to  
111 evaluate the effect of granulometric fractionation followed by micronization of OP on the  
112 biotransformation of phenolic compounds in an *in vitro* static model of colonic  
113 fermentation with human feces.

114

## 115 **2. Materials and methods**

### 116 **2.1. Olive pomace**

117         The OP from *Olea europaea* cv. 'Arbequina' was collected immediately after olive  
118 oil extraction by the two-phase continuous extraction process, in an extra virgin olive oil  
119 industry located in the city of Formigueiro, Rio Grande do Sul state, Brazil (29° 59' 01"  
120 S; 53° 21' 50 " W).

121

### 122 **2.2. Granulometric fractionation and micronization of olive pomace**

123         The crude sample of OP was submitted to granulometric fractionation at 2-mm  
124 sieve, as described below, to obtain a fraction that was named granulometrically

125 fractionated OP (GF). GF was submitted to micronization to obtain a fraction that was  
126 named granulometrically fractionated and micronized OP (GFM), as described below.  
127 OP without physical modification was lyophilized in a freeze dryer (LS 3000, Terroni  
128 Equipamentos Científicos, SP, Brazil), crushed in a knife mill (MA 630, Marconi®, SP,  
129 Brazil) and identified as non-fractionated OP (NF).

130 Crude OP was subjected to granulometric fractionation with a 2-mm sieve as  
131 described by Speroni et al. (2019), and the fraction with particle size < 2-mm was  
132 centrifuged ( $1774 \times g$  for 10 min), the sediment was collected, lyophilized in a freeze  
133 dryer (LS 3000, Terroni Equipamentos Científicos, SP, Brazil), crushed in a knife mill  
134 (MA 630, Marconi®, SP, Brazil) and degreased with *n*-hexane, according to Goulart et  
135 al. (2013). This fraction was identified as GF.

136 Thereafter, GF was micronized in a planetary ball mill (PM 100, Retsch Co.,  
137 Haan, Germany), using a 250 mL container with six stainless steel balls (30 mm diameter  
138 each). The milling time was optimized by Speroni et al. (2020), with 15 g of sample  
139 ground at  $300 \text{ r min}^{-1}$  for 5 h, with a 2 min pause every 10 min of grinding. After  
140 micronization, the sample was identified as GFM.

141

### 142 **2.3. Particle size analysis**

143 Particle size was assessed in a Laser Diffraction Particle Size Analyzer (model LS  
144 13320, Beckman Coulter, FL, USA) following the manufacturer instructions. Triplicate  
145 samples were added to the equipment until optimal obscuration was achieved in the  
146 software. Thereafter, the powders were dispersed in an aqueous medium and submitted  
147 to an ultrasound treatment for 1 min inside the equipment before analysis.

148

### 149 **2.4. *In vitro* simulation of gastrointestinal digestion**

150 Samples of NF, GF and GFM (proximate composition shown in Table S1,  
151 supplementary material) were submitted to a simulated gastrointestinal digestion based  
152 on the standardized INFOGEST 2.0 *in vitro* digestion method (Brodkorb et al., 2019).  
153 The samples are subjected to digestion under conditions that sequentially mimic the oral,  
154 gastric and intestinal stages (Fig. 1) with amounts of electrolytes, enzymes, bile, dilution,  
155 pH and digestion time based on the physiology of the gastrointestinal tract. The conditions  
156 were based on the study of Brodkorb et al. (2019) with the following modifications: the  
157 oral phase did not include amylase because OP is not a starchy food, lipase was not  
158 included in the gastric phase because OP was defatted before micronization, and the  
159 bioaccessible fraction was separated by dialysis during the intestinal phase.

160 For the oral phase, 4 g of each sample (NF, GF and GFM) were separately  
161 incubated (without amylase) with salivary fluid pH 7.0 at 37 °C for 2 min on a rotary  
162 shaker (AGROT-BI, IONLAB, PR, Brazil). Subsequently, for the gastric phase, the pH  
163 was corrected to 3, by adding gastric fluid and pepsin (2000 U/mL; P7000, Sigma-  
164 Aldrich, MO, USA) in a final volume of 20 mL, followed by incubation at 37 °C in the  
165 rotary shaker for 2 h. In the intestinal phase, the pH was adjusted to 7, the intestinal fluid,  
166 bile salts with sodium deoxycholate and sodium cholate (10 mM; C6750 and C1254,  
167 Sigma Aldrich, MO, USA) and pancreatin (100 U/mL; P7545, Sigma Aldrich, MO, USA)  
168 were added in a final volume of 40 mL. This solution was transferred to a dialysis  
169 membrane (12400 Da; D0530, Sigma Aldrich, MO, USA) that was placed in a beaker  
170 containing 200 mL of phosphate buffer (24.9 mM, pH 7.4) and intestinal incubation was  
171 performed for 2 h at 37 °C with sporadic shaking. The membrane was previously activated  
172 as described by Dutra et al. (2017). The fraction that remained inside the dialysis  
173 membrane after intestinal digestion (IN-NF, IN-GF and IN-GFM) represents the fraction  
174 that is not available for absorption, and will reach the colon, whereas the fraction that was



175 able to cross the dialysis membrane (OUT-NF, OUT-GF and OUT-GFM) represents the  
176 bioaccessible fraction. The OUT fraction was used for another study, whereas the IN  
177 fractions were lyophilized and used for colonic fermentation with human feces.

178

## 179 **2.5 Static model of colonic fermentation *in vitro***

180 The protocol was approved by the Ethics Committee of the Federal University of  
181 Santa Maria (CAAE 20528819.4.0000.5346). Eighteen healthy volunteers (18-55 years,  
182 2 males, 16 females) were included as fecal donors in this study. Exclusion criteria were  
183 chronic, infectious, or gastrointestinal diseases or those who had received antibiotic  
184 treatment in the last 6 months. Twenty stool samples were collected and used to perform  
185 five independent fermentation assays. Each assay was performed with a pool of feces  
186 from four donors. Each donor made a single fecal donation, except for two donors that  
187 donated twice. Feces were used within 2 h after defecation and kept at room temperature  
188 under anaerobic conditions (N<sub>2</sub>) until the time of the experiment.

189 Colonic fermentation was mimicked using the nutrient base medium described by  
190 Ribeiro et al. (2021). Equal amounts of fecal samples from 4 donors were pooled and  
191 homogenized in the nutrient base medium at a ratio of 0.5:10 m/v. The fecal suspension  
192 was filtered through sterile gauze under anaerobic conditions (N<sub>2</sub>) and then used for the  
193 fermentation assay. The fecal inoculum buffer was purged with N<sub>2</sub> for 30 s in each  
194 fermentation tube to remove O<sub>2</sub>.

195 Samples (0.25 g of IN-NF, IN-GF and IN-GFM) were incubated with 25 mL of  
196 fecal inoculum buffer at 37 °C for 0, 2, 8, 24 and 48 h in autoclaved Falcon tubes closed  
197 with rubber stoppers that allow excess gas to escape (Ribeiro et al., 2021). Separate flasks  
198 were used for each fermentation time and the pH was determined at the end of each  
199 incubation time. During the adjustment of the experimental conditions for colonic

200 fermentation, the fecal inoculum was incubated with 0.25 g inulin as a positive control to  
201 prove the viability of fecal inoculum in the fermentation assay. Thereafter, during the  
202 experimental stage, two control fermentation runs were carried out in parallel with  
203 samples. Control 1 was then composed of 0.25 g of IN-NF, IN-GF and IN-GFM samples  
204 that were incubated with buffer solution, in the absence of feces and was used to evaluate  
205 the chemical degradation of phenolic compounds, independent of the microbiota. Control  
206 2 was the fecal inoculum buffer without the inclusion of IN samples and was used to  
207 account for the phenolic compounds that were already found in the feces. The phenolic  
208 content found in control 2 was always subtracted from the phenolic content found in the  
209 fermentation assays of IN-NF, IN-GF and IN-GFM. After the end of fermentation,  
210 samples were centrifuged at  $1,400 \times g$  for 10 min and the supernatant was immediately  
211 frozen under liquid N<sub>2</sub> and stored at -20 °C.

212

## 213 **2.6 pH analysis**

214 The pH value was determined immediately after finishing colonic fermentation  
215 assays, using a digital potentiometer (P1000, PHOX Suprimentos Científicos, Paraná,  
216 Brazil).

217

## 218 **2.7 Extraction of phenolic compounds from colonic fermentation assay**

219 Aliquots of supernatant samples obtained after fermentation (6 mL) were  
220 extracted using an acidified acetone solution (0.35% formic acid, v/v; 7 mL) according to  
221 Quatrin et al. (2020). After vortex mixing for 1 min, samples were centrifuged at  $1,100 \times$   
222 g for 10 min to collect the supernatant. The organic solvent was removed in a rotary  
223 evaporator ( $38 \pm 2$  °C) and the extract was filtered on a 0.22- $\mu\text{m}$  polytetrafluoroethylene  
224 filter.

225

## 226 **2.8 Identification and quantification of phenolic compounds**

227 Phenolic compounds were identified and quantified using an ultra high-  
228 performance liquid chromatograph (Nexera XR, Shimadzu, Kyoto, Japan) coupled to a  
229 triple-quadrupole mass spectrometer (UHPLC-MS/MS) (LCMS-8045, Shimadzu, Kyoto,  
230 Japan) equipped with a binary pump, degasser, communication module, oven column and  
231 automatic injector. Samples were injected (10  $\mu$ L) onto a Zorbax RRHD Eclipse XDB-  
232 C18 analytical column (4.6 mm x 150 mm, 1.8  $\mu$ m particle size; Agilent Technologies,  
233 CA, USA) at 35 °C. The mobile phase was HPLC grade water obtained from a Direct-  
234 Q® 3 UV equipment (Merck Millipore, Darmstadt, Germany) with 0.5% acetic acid  
235 (eluent A) and acetonitrile (eluent B) at 0.2 mL min<sup>-1</sup>. Chromatographic separation was  
236 carried out in a reverse-phase mode according to the following multistep elution gradient,  
237 adapted from Abu-Reidah, Arráez-Román, Al-Nuri, Warad, & Segura-Carretero, (2019):  
238 0% B from 0 to 7 min; 10% B from 7 to 11 min; 14% B from 11 to 17 min; 18% B from  
239 17 to 20 min; 20% B from 20 to 21 min; 27% B from 21 to 22 min; 29% B from 22 to 23  
240 min; 30% B from 23 to 33 min; 36% B from 33 to 40 min. Phenolic compounds were  
241 monitored in the multiple reaction monitoring spectrum mode at conditions optimized  
242 using authentic phenolic standards. The equipment was operated with an electrospray  
243 ionization source (ESI) under the following conditions: interface temperature at 350 °C,  
244 heating gas flow at 6 L min<sup>-1</sup>, nebulizing gas flow at 2 L min<sup>-1</sup>, drying gas flow at 4 L  
245 min<sup>-1</sup>, interface voltage at -3.5 V. Analytical curves were constructed using commercial  
246 standards of verbascoside (Chromadex, CO, USA), protocatechuic acid, 3-  
247 hydroxytyrosol, 4-hydroxybenzoic acid, tyrosol, caffeic acid, vanillic acid, homovanillic  
248 acid, *p*-coumaric acid, ferulic acid, oleuropein, luteolin and apigenin (Sigma-Aldrich,  
249 MO, USA). Phenolic compounds were quantified using authentic reference standards

250 except for hydroxytyrosol-glycoside that was quantified as equivalents of hydroxytyrosol  
251 and oleuropein aglycone that was quantified as equivalents of oleuropein. Validation data  
252 for the analysis of phenolic compounds is shown in Table S2 (supplementary material).

253

## 254 **2.9 Statistical analysis**

255 All statistical evaluations were performed using GraphPad Prism version 5.0 for  
256 Windows (GraphPad Software, CA, USA). The data were expressed as mean  $\pm$  standard  
257 error of the mean (S.E.M.). Data on the profile of phenolic compounds during  
258 fermentation were analyzed by factorial analyses of variance (5 fermentation times  $\times$  3  
259 OP-IN samples) with the fermentation time treated as a repeated measure. Duncan's test  
260 was used for *post hoc* comparison when analysis of variance revealed a significant main  
261 effect or interaction between factors.

262

## 263 **3. Results and discussion**

### 264 **3.1 Particle size**

265 The average particle size of NF decreased after granulometric fractionation (GF)  
266 and micronization (GFM), as shown in Fig. S1 (supplementary material). Powdered  
267 samples obtained from OP without physical modification (NF) had a wide distribution  
268 range for the particle size, reaching values over 1800  $\mu\text{m}$ , with an average size of 320.8  
269  $\pm$  195.0  $\mu\text{m}$  (mean  $\pm$  standard deviation). This occurred mainly due to the presence of  
270 large particles of stones and pulp that are difficult to grind in conventional knife milling  
271 devices.

272 The average particle size of powdered OP samples was reduced by granulometric  
273 fractionation using a 2-mm sieve (GF) (mean  $\pm$  standard deviation: 143.0  $\pm$  5.3  $\mu\text{m}$ ) and  
274 even more reduced when samples were subsequently micronized (GFM) (mean  $\pm$

275 standard deviation:  $22.4 \pm 0.9 \mu\text{m}$ ). As previously demonstrated by our research group,  
276 long-time (5 h) micronization, as the one used in the present study, standardizes the  
277 particle size as indicated by the great decrease in the standard deviation of particle size  
278 values (Speroni et al., 2020).

279

### 280 **3.2 pH and fermentation parameters**

281 GFM samples had a small decrease in pH values during fermentation (pH 7.22  
282 at 0 h vs. pH 6.95 at 48 h), with a significant difference from the Control 2 (fermentation  
283 of feces without OP) at 8, 24, and 48 h. The pH of GF was also reduced during  
284 fermentation (pH 7.21 at 0 h vs. pH 6.96 at 48 h) and significantly lower than Control 2  
285 at 24 h and 48 h ( $p < 0.05$ ), as shown in Fig. S2 (supplementary material).

286 The reduction of pH is associated to the production of short chain fatty acids,  
287 which is expected to increase during intestinal fermentation with viable fecal microbiota  
288 and enough amount of fermentable substrates (Tejada-Ortigoza et al., 2022). The viability  
289 of fecal microbiota used in this study was demonstrated by the inclusion of a positive  
290 control that contained a high content of inulin (fermentable carbohydrate) and resulted in  
291 a pH drop from 8.29 to 5.15 (data not shown). Thus, the small pH drop observed during  
292 the final fermentation assay was not caused by low microbial viability but was rather  
293 related to the composition of the nutrient base medium (Ribeiro et al., 2021) and that of  
294 the OP samples (Table S1, supplementary material) which resulted in low amount of  
295 fermentable substrates. This low fermentative activity did not affect our results that were  
296 focused on the biotransformation of phenolic compounds.

297

### 298 **3.3 Transformation of phenolic compounds during colonic fermentation**

299           The concentration of phenolic compounds in OP samples during fermentation  
300 was corrected to eliminate the interference of phenolic compounds already present in the  
301 feces (Control 2). The sum of phenolic compounds was high in the start of colonic  
302 fermentation assay (time 0), especially in GFM (146.7 mg 100 g<sup>-1</sup> d.b.) compared to NF  
303 and GF (31.1 and 85.5 mg 100 g<sup>-1</sup> d.b.) (Table S3, supplementary material). The  
304 fractionation of OP followed by micronization resulted in lower particle size that likely  
305 facilitated the release of phenolic compounds bound to the matrix yielding greater  
306 amounts of phenolic compounds during the colonic fermentation of GFM than in GF and  
307 NF.

308           Hydroxytyrosol is the main phenolic alcohol found in OP (Ribeiro et al., 2020).  
309 Hydroxytyrosol has high bioaccessibility in the salivary, gastric and intestinal phases  
310 during *in vitro* digestion and it is still found in the insoluble fraction that reaches the colon  
311 (Speroni et al., 2021). Granulometric fractionation of OP followed by micronization  
312 significantly increased the amount of hydroxytyrosol released during *in vitro*  
313 gastrointestinal digestion (Speroni et al., 2021). At the start of fermentation (0 h) the  
314 concentration of hydroxytyrosol (mg 100 g<sup>-1</sup> of sample d.b.) was higher in GFM (15.2 ±  
315 2.0) and GF (8.1 ± 0.9) than in NF (3.0 ± 0.2) (Fig. 2A; Table S3, supplementary  
316 material). The concentration of hydroxytyrosol released during colonic fermentation  
317 increased for all OP samples during the first hours, reached a peak at 8 h, and thereafter  
318 decreased from 24 h onwards ( $p<0.05$ ; Fig. 2A). GF and GFM released higher  
319 hydroxytyrosol levels than NF after 2 (4.8x and 7.9x, respectively), 8 (2.6x and 3.8x,  
320 respectively) and 24 h (2x and 1.6x, respectively) of fermentation ( $p<0.05$ ; Fig. 2A).  
321 Additionally, hydroxytyrosol levels released by GFM were higher than GF at 2 and 8 h  
322 of fermentation ( $p<0.05$ ; Fig. 2A). At 48 h of fermentation, small amounts of  
323 hydroxytyrosol were found regardless of the sample, demonstrating the complete

324 metabolism of the compound and in agreement with a recent study on OP fermentation  
325 (Ribeiro et al., 2021).

326 Hydroxytyrosol-glycoside represents 36 - 60% of the phenolic compounds found  
327 in the digested NF, GF and GFM samples that were used for colonic fermentation (time  
328 0 h, Table S3, supplementary material). In addition, at the start of fermentation (0 h) there  
329 was a significant difference in the levels of hydroxytyrosol-glycoside among samples:  
330 GFM > GF > NF ( $p < 0.05$ ; Fig. 2B). This data corroborates the effectiveness of  
331 micronization to improve the release of phenolic alcohols and related compounds, and  
332 agrees with our previous study on the gastrointestinal digestion of OP up to the small  
333 intestinal phase (Speroni et al., 2021). However, hydroxytyrosol-glycoside was detected  
334 at trace levels after 2 h of fermentation. The parallel increase in the levels of  
335 hydroxytyrosol indicates a rapid and extensive metabolism of hydroxytyrosol-glycoside  
336 by fecal microbiota that removes the sugar moiety favoring the increase of aglycone levels  
337 (Fig. 2A).

338 The most remarkable effect of OP fractionation followed by micronization  
339 (GFM) was the significant increase in the release of tyrosol during colonic fermentation  
340 compared to NF and GF, in which the presence of this compound was not detected  
341 ( $p < 0.05$ ; Fig 2C). The increase in tyrosol levels of GFM from 0 to 2 h is likely related to  
342 the metabolism of hydroxytyrosol by intestinal microbiota (Fig. 2), which follows the  
343 biotransformation pathway depicted in Fig. 3. Although GFM keeps much higher levels  
344 of tyrosol than NF and GF up to 24 h ( $p < 0.05$ ), a progressive decrease was observed from  
345 2 h onwards and culminates with the disappearance of tyrosol at 48 h (Fig. 2C). The main  
346 metabolites generated from the microbial transformation of phenolic alcohols, such as  
347 hydroxytyrosol and tyrosol, are homovanillic acid, phenylacetic acid and its derivatives,  
348 and vanillyl alcohol (Ribeiro et al., 2021; López de Las Hazas et al., 2016) (Fig. 3). Only

349 homovanillic acid was monitored in the present study. Its levels progressively increased  
350 during the colonic fermentation of OP samples (Fig. 2D), which agrees with the study by  
351 Ribeiro et al. (2021), but no difference was observed among NF, GF or GFM samples.  
352 The presence of this compound was also reported by Conterno et al. (2019), who  
353 quantified homovanillic acid in the plasma of volunteers after feeding with cookies made  
354 from OP.

355 Oleuropein is the main phenolic glycoside found in olive fruits, but it is  
356 extensively degraded during olive oil extraction generating phenolic alcohols that are the  
357 major phenolics in OP (Pedan et al., 2019). Thus, small amounts of secoiridoids, such as  
358 oleuropein and its derivatives, have been reported in OP (López de Las Hazas et al.,  
359 2016). In the present study, only trace amounts of these compounds were detected in NF  
360 samples at the start of fermentation (Fig. 4). Micronized OP has been shown to have a  
361 greater release of oleuropein during the salivary and gastric phases of digestion, but  
362 oleuropein was still found in the fraction that was not accessible for intestinal absorption,  
363 which is the one that will be available for biotransformation by the intestinal microbiota  
364 after reaching the colon (Speroni et al., 2021). In the present investigation, oleuropein  
365 was found only at the initial fermentation time (0 h) in GFM and it was completely  
366 degraded up to 2 h ( $p<0.05$ ; Fig. 4A). The degradation of oleuropein follows the  
367 biotransformation pathway depicted in Fig. 3, leading to the increase of oleuropein  
368 aglycone, as depicted in Fig. 4B. Granulometric fractionation associated or not to  
369 micronization (GFM and GF), were effective to increase the release of oleuropein  
370 aglycone at the start of fermentation (up to 2 h) compared to NF ( $p<0.05$ ), which released  
371 only trace amounts of this compound (Fig. 4B). After 2 h of fermentation, oleuropein  
372 aglycone was rapidly degraded in GF and GFM samples. After 8h of fermentation  
373 oleuropein aglycone was not detected, as observed by Mosele et al. (2014), who detected



374 elenolic acid and oleuropein aglycone at low amounts in the initial times decreasing to  
375 trace levels at 12 h of fermentation.

376 Luteolin and apigenin are the main flavonoids in OP. They show good stability  
377 during simulated *in vitro* digestion, which results in a quite high proportion of their intake  
378 dose reaching the colon (43.1% for luteolin and 85.2% for apigenin in GF) (Speroni et  
379 al., 2021). Luteolin concentration was high in the OP samples at the initial fermentation  
380 time (Fig. 5A), but it was rapidly reduced up to 8 h, when it was found at trace levels. No  
381 difference was observed in luteolin levels among OP samples. Apigenin had a similar  
382 time-course behavior compared to luteolin but GFM and GF released higher apigenin  
383 amounts than NF up to 2 h of fermentation ( $p<0.05$ , Fig. 5B). The rapid degradation of  
384 these flavonoids is likely related to their deglycosylation by microbial action (Mosele et  
385 al., 2015).

386 Among the phenolic acids found in fraction of OP that reaches the colon, the  
387 derivatives of hydroxybenzoic acid, namely protocatechuic, vanillic and 4-  
388 hydroxybenzoic acids, showed an increase up to 8 h of fermentation (Fig. 6A, B, C).  
389 Thereafter, the levels of protocatechuic and vanillic acid were decreased, whereas 4-  
390 hydroxybenzoic acid remained at a plateau up to 48 h of fermentation (Fig. 6). GF (at 2  
391 h) and GFM (at 2, 8 and 24 h) had higher protocatechuic acid levels than NF during  
392 fermentation ( $p<0.05$ ; Fig 6A). GF and GFM also had higher levels of vanillic acid than  
393 NF during fermentation (at 2 and 8 h,  $p<0.05$ ; Fig. 6B). The levels of 4-hydroxybenzoic  
394 acid did not differ among OP samples during fermentation (Fig. 6C). These metabolites  
395 are described by Mosele et al. (2015), as end products of flavonoid fermentation.  
396 Accordingly, the increase in hydroxybenzoic acid derivatives up to 8 h of fermentation  
397 was associated with the degradation of luteolin and apigenin (Fig 5). Fractionation and  
398 micronization increased the release of these hydroxybenzoic acid derivatives which will

399 favor their absorption. The particle size reduction likely favored microbial metabolic  
400 activity in the OP matrix.

401 Hydroxycinnamic acid derivatives, such as *p*-coumaric and caffeic acid, had  
402 their levels decreased during fermentation being found at trace levels from 8 h onwards.  
403 At 0 h, *p*-coumaric and caffeic acid levels were higher for GFM and GF than NF, whereas  
404 at 2 h of fermentation the levels were higher for GFM than for GF and NF ( $p<0.05$ ; Fig.  
405 6D and 6E).

406 A major finding of the study is that GF and at a greater degree GFM increased  
407 the amount of phenolic compounds released during the colonic fermentation and  
408 sustained higher levels of phenolic compounds than NF up to 24 h of colonic  
409 fermentation. It was remarkable that GF and GFM increased the colonic levels of  
410 hydroxytyrosol, hydroxytyrosol glycoside, oleuropein aglycone, apigenin and phenolic  
411 acid metabolites in the first hours of colonic fermentation compared to the non-modified  
412 OP, whereas GFM caused an even greater increase of hydroxytyrosol and tyrosol  
413 compared to GF. These findings are particularly relevant because they reveal that  
414 granulometric fractionation followed by micronization is able improve the nutraceutical  
415 potential of OP. In fact, hydroxytyrosol and tyrosol have been shown to exhibit  
416 cardioprotective, anticancer and neuroprotective effects (Marković et al., 2019;  
417 Rodríguez-López et al., 2020), whereas hydroxytyrosol has been demonstrated to  
418 attenuate insulin resistance and obesity through the modulation of gut microbiota (Liu et  
419 al., 2019).

420

#### 421 **4. Conclusions**

422 Parallel to the reduction in particle size, granulometric fractionation followed by  
423 micronization increased the amount of phenolic compounds in the fraction of OP that

424 reaches the colon. The increased surface area of the OP modified by granulometric  
425 fractionation or by granulometric fractionation followed by micronization favored the  
426 release of hydroxytyrosol, oleuropein aglycone, apigenin and phenolic acid metabolites  
427 in the first hours of colonic fermentation compared to the non-modified OP.  
428 Hydroxytyrosol (8 h) and tyrosol (2 h) were the compounds that reached the highest  
429 concentration and highest stability during simulated colonic fermentation. Granulometric  
430 fractionation followed by micronization of OP caused higher release of hydroxytyrosol  
431 than granulometric fractionation alone. Moreover, granulometric fractionation followed  
432 by micronization was the only process that resulted in the release of tyrosol during colonic  
433 fermentation and allowed relatively high tyrosol levels to be sustained up to 24 h of  
434 fermentation. Oleuropein was found only in the OP that was modified by granulometric  
435 fractionation followed by micronization being completely degraded into oleuropein  
436 aglycone within 2 h of fermentation. The final metabolites formed were homovanillic  
437 acid and hydroxybenzoic acids, such as vanillic, protocatechuic and hydroxybenzoic acid.  
438 These data confirm the hypothesis that micronization of OP enhances the amount of  
439 phenolic compounds released during colonic fermentation and support the conclusion that  
440 micronization associated to granulometric fractionation was more efficient than  
441 granulometric fractionation alone to increase the release of phenolic compounds from the  
442 OP matrix during simulated colonic fermentation. *In vivo* assays are needed to confirm  
443 the bioavailability of phenolic compounds and the effect on the gut microbiota to further  
444 corroborate the health benefits of micronized OP.

445

#### 446 **CRedit authorship contribution statement**

447 **Camila Sant'Anna Monteiro:** Investigation, Methodology, Data curation,  
448 Conceptualization, Writing - original draft, Writing - review & editing, Visualization.

449 **Paula Colpo Bortolazzo:** Investigation, Methodology, Visualization, Data acuration.  
450 **Camila Araujo Amorim Bonini:** Investigation, Visualization, Methodology. **Luana**  
451 **Tamires Dluzniewski:** Investigation, Visualization. **Dariane Trivisiol da Silva:**  
452 Investigation, Methodology. **Julia Baranzelli:** Formal analysis, Visualization,  
453 Methodology. **Franciele Aline Smaniotto:** Investigation, Visualization, Methodology.  
454 **Cristiano Augusto Ballus:** Writing - review & editing, Methodology. **Jesús Lozano-**  
455 **Sánchez:** Writing - review & editing, Formal analysis. **Sabrina Somacal:** Investigation,  
456 Writing - review & editing, Data curation, Visualization. **Tatiana Emanuelli:**  
457 Conceptualization, Resources, Supervision, Writing – original draft, Writing - review &  
458 editing, Funding acquisition, Project administration.

459

#### 460 **Conflict of interest**

461 Authors declare no conflict of interest.

462

#### 463 **Acknowledgments**

464 This study was supported by CNPq (Conselho Nacional de Desenvolvimento Científico  
465 e Tecnológico) [grant numbers 435932/2018-7; 303654/2017-1; 422700/2021-5],  
466 CAPES (Coordenação de Aperfeiçoamento Pessoal de Nível Superior) [Finance code  
467 001] and Secretaria de Desenvolvimento Econômico, Ciência e Tecnologia do Estado do  
468 Rio Grande do Sul [grant number DCIT 41/2017]. We thank to Olivais da Fonte Company  
469 (Formigueiro, RS, Brazil) for the kind donation of olive pomace.

470

#### 471 **References**

472 Abu-Reidah, I. M., Arráez-Román, D., Al-Nuri, M., Warad, I., & Segura-Carretero, A.  
473 (2019). Untargeted metabolite profiling and phytochemical analysis of *Micromeria*  
474 *fruticosa* L. (*Lamiaceae*) leaves. *Food Chemistry*, 279, 128–143.

475 <https://doi.org/10.1016/j.foodchem.2018.11.144>

476 Augusti, P. R., Conterato, G. M. M., Denardin, C. C., Prazeres, I. D., Serra, A. T.,  
477 Bronze, M. R., & Emanuelli, T. (2021). Bioactivity, bioavailability, and gut microbiota  
478 transformations of dietary phenolic compounds: implications for COVID-19. *Journal of*  
479 *Nutritional Biochemistry*, 97, 108787. <https://doi.org/10.1016/j.jnutbio.2021.108787>

480 Brodkorb, A., Egger, L., Alminger, M., Alvito, P., Assunção, R., Ballance, S., Bohn, T.,  
481 Bourlieu-Lacanal, C., Boutrou, R., Carrière, F., Clemente, A., Corredig, M., Dupont, D.,  
482 Dufour, C., Edwards, C., Golding, M., Karakaya, S., Kirkhus, B., Le Feunteun, S., ...  
483 Recio, I. (2019). INFOGEST static *in vitro* simulation of gastrointestinal food digestion.  
484 *Nature Protocols*, 14, 991–1014. <https://doi.org/10.1038/s41596-018-0119-1>

485 Chen, T., Zhang, M., Bhandari, B., & Yang, Z. (2018). Micronization and nanosizing of  
486 particles for an enhanced quality of food: A review. *In Critical Reviews in Food Science*  
487 *and Nutrition*, 58, 993-1001. <https://doi.org/10.1080/10408398.2016.1236238>

488 Conterno, L., Martinelli, F., Tamburini, M., Fava, F., Mancini, A., Sordo, M., Pindo,  
489 M., Martens, S., Masuero, D., Vrhovsek, U., Dal Lago, C., Ferrario, G., Morandini, M.,  
490 & Tuohy, K. (2019). Measuring the impact of olive pomace enriched biscuits on the gut  
491 microbiota and its metabolic activity in mildly hypercholesterolaemic subjects.  
492 *European Journal of Nutrition*, 58, 63–81. <https://doi.org/10.1007/s00394-017-1572-2>

493 Covas, M. I., de la Torre, K., Farré-Albaladejo, M., Kaikkonen, J., Fitó, M., López-  
494 Sabater, C., Pujadas-Bastardes, M. A., Joglar, J., Weinbrenner, T., Lamuela-Raventós,  
495 R. M., & de la Torre, R. (2006). Postprandial LDL phenolic content and LDL oxidation  
496 are modulated by olive oil phenolic compounds in humans. *Free Radical Biology &*  
497 *Medicine*, 40, 608–616. <https://doi.org/10.1016/j.freeradbiomed.2005.09.027>

498 Dermeche, S., Nadour, M., Larroche, C., Moulti-Mati, F., & Michaud, P. (2013). Olive  
499 mill wastes: Biochemical characterizations and valorization strategies. *Process*  
500 *Biochemistry*, 48, 1532–1552. <https://doi.org/10.1016/j.procbio.2013.07.010>

501 Dhiman, A., & Prabhakar, P. K. (2021). Micronization in food processing: A  
502 comprehensive review of mechanistic approach, physicochemical, functional properties  
503 and self-stability of micronized food materials. *Journal of Food Engineering*, 292,  
504 110248. <https://doi.org/10.1016/j.jfoodeng.2020.110248>

505 Dutra, R. L. T., Dantas, A. M., Marques, D. A., Batista, J. D. F, Meireles, B. R. L. A.,  
506 Cordeiro, A. M. T. M., Magnani, M., & Borges, G. S. C. (2017). Bioaccessibility and  
507 antioxidant activity of phenolic compounds in frozen pulps of Brazilian exotic fruits  
508 exposed to simulated gastrointestinal conditions. *Food Research International*, 100,  
509 650–657. <https://doi.org/10.1016/j.foodres.2017.07.047>

510 Gil-Sánchez, I., Cueva, C., Sanz-Buenhombre, M., Guadarrama, A., Moreno-Arribas,  
511 M. V., & Bartolomé, B. (2018). Dynamic gastrointestinal digestion of grape pomace  
512 extracts: Bioaccessible phenolic metabolites and impact on human gut microbiota.  
513 *Journal of Food Composition and Analysis*, 68, 41–52.  
514 <https://doi.org/10.1016/j.jfca.2017.05.005>

515 Goulart, F. R., Speroni, C. S., Lovatto, N. D. M., Loureiro, B. B., Corrêia, V., Neto, J.  
516 R., & Picolli, L. (2013). Activity of digestive enzymes and growth parameters of  
517 juvenile jundiá (*Rhandia quelen*) fed linseed meal in nature and demucilaged. *Semina:  
518 Ciências Agrárias*, 34, 3069–3080. <https://doi.org/10.5433/1679-0359.2013v34n6p3069>

519 Li, Y., Li, M., Wang, L., & Li, Z. (2022). Effect of particle size on the release behavior  
520 and functional properties of wheat bran phenolic compounds during *in vitro*  
521 gastrointestinal digestion. *Food Chemistry*, 367, 130751.  
522 <https://doi.org/10.1016/j.foodchem.2021.130751>

523 Liu, Z., Wang, N., Ma, Y., & Wen, D. (2019). Hydroxytyrosol improves obesity and  
524 insulin resistance by modulating gut microbiota in high-fat diet-induced obese mice.  
525 *Frontiers in Microbiology*, 10, 390. <https://doi.org/10.3389/fmicb.2019.00390>

526 López de las Hazas, M. C., Piñol, C., Macià, A., Romero, M. P., Pedret, A., Solà, R.,  
527 Rubió, L., & Motilva, M. J. (2016). Differential absorption and metabolism of  
528 hydroxytyrosol and its precursors oleuropein and secoiridoids. *Journal of Functional  
529 Foods*, 22, 52–63. <https://doi.org/10.1016/j.jff.2016.01.030>

530 Malapert, A., Reboul, E., Loonis, M., Dangles, O., & Tomao, V. (2018). Direct and  
531 rapid profiling of biophenols in olive pomace by UHPLC-DAD-MS. *Food Analytical  
532 Methods*, 11, 1001–1010. <https://doi.org/10.1007/s12161-017-1064-2>

533 Marković, A.K.; Torić, J.; Barbarić, M.; Brala, C. J. (2019). Hydroxytyrosol, tyrosol  
534 and derivatives and their potential effects on human health. *Molecules*, 24, 2001.  
535 <https://doi.org/10.3390/molecules24102001>

536 Mosele, J. I., Macià, A., & Motilva, M. J. (2015). Metabolic and microbial modulation  
537 of the large intestine ecosystem by non-absorbed diet phenolic compounds: A review.  
538 *Molecules*, 20, 17429–17468. <https://doi.org/10.3390/molecules200917429>

539 Mosele, J. I., Martín-Peláez, S., Macià, A., Farràs, M., Valls, R. M., Catalán, Ú., &  
540 Motilva, M. J. (2014). Faecal microbial metabolism of olive oil phenolic compounds: *In*  
541 *vitro* and *in vivo* approaches. *Molecular Nutrition & Food Research*, 58, 1809–1819.  
542 <https://doi.org/10.1002/mnfr.201400124>

543 Pedan, V., Popp, M., Rohn, S., Nyfeler, M., & Bongartz, A. (2019). Characterization of  
544 phenolic compounds and their contribution to sensory properties of olive oil. *Molecules*,  
545 24, 2041. <https://doi.org/10.3390/molecules24112041>

546 Quatrin, A., Rampelotto, C., Pauletto, R., Maurer, L. H., Nichelle, S. M., Klein, B.,  
547 Rodrigues, R. F., Maróstica Junior, M. R., Fonseca, B. de S., de Menezes, C. R., Mello,  
548 R. de O., Rodrigues, E., Bochi, V. C., & Emanuelli, T. (2020). Bioaccessibility and  
549 catabolism of phenolic compounds from jaboticaba (*Myrciaria trunciflora*) fruit peel  
550 during *in vitro* gastrointestinal digestion and colonic fermentation. *Journal of*  
551 *Functional Foods*, 65, 103714. <https://doi.org/10.1016/j.jff.2019.103714>

552 Ribeiro, T. B., Costa, C. M., Bonifácio-Lopes, T., Silva, S., Veiga, M., Monforte, A. R.,  
553 Nunes, J., Vicente, A. A., & Pintado, M. (2021). Prebiotic effects of olive pomace  
554 powders in the gut: *In vitro* evaluation of the inhibition of adhesion of pathogens,  
555 prebiotic and antioxidant effects. *Food Hydrocolloids*, 112, 106312.  
556 <https://doi.org/10.1016/j.foodhyd.2020.106312>

557 Ribeiro, T. B., Oliveira, A., Campos, D., Nunes, J., Vicente, A. A., & Pintado, M.  
558 (2020). Simulated digestion of an olive pomace water-soluble ingredient: relationship  
559 between the bioaccessibility of compounds and their potential health benefits. *Food &*  
560 *Function*, 11, 2238–2254. <https://doi.org/10.1039/C9FO03000J>

561 Rocchetti, G., Senizza, B., Giuberti, G., Montesano, D., Trevisan, M., & Lucini, L.  
562 (2020). Metabolomic study to evaluate the transformations of extra-virgin olive oil's  
563 antioxidant phytochemicals during *in vitro* gastrointestinal digestion. *Antioxidants*, 9, 1–  
564 15. <https://doi.org/10.3390/antiox9040302>

565 Rodríguez-López, P., Lozano-Sánchez, J., Borrás-Linares, I., Emanuelli, T., Menéndez,  
566 J. A., & Segura-Carretero, A. (2020). Structure–biological activity relationships of

567 extra-virgin olive oil phenolic compounds: Health properties and bioavailability.  
568 *Antioxidants*, 9, 1–17. <https://doi.org/10.3390/antiox9080685>

569 Serreli, G., & Deiana, M. (2018). Biological relevance of extra virgin olive oil  
570 polyphenols metabolites. *Antioxidants*, 7, 11–13. <https://doi.org/10.3390/antiox7120170>

571 Shu, Y., Li, J., Yang, X., Dong, X., & Wang, X. (2019). Effect of particle size on the  
572 bioaccessibility of polyphenols and polysaccharides in green tea powder and its  
573 antioxidant activity after simulated human digestion. *Journal of Food Science and*  
574 *Technology*, 56, 1127–1133. <https://doi.org/10.1007/s13197-019-03573-4>

575 Speroni, C. S., Bender, A. B. B., Stiebe, J., Ballus, C. A., Ávila, P. F., Goldbeck, R.,  
576 Morisso, F. D. P., Silva, L. P. da, & Emanuelli, T. (2020). Granulometric fractionation  
577 and micronization: A process for increasing soluble dietary fiber content and improving  
578 technological and functional properties of olive pomace. *LWT*, 130, 109526.  
579 <https://doi.org/10.1016/j.lwt.2020.109526>

580 Speroni, C. S., Guerra, D. R., Bender, A. B. B., Stiebe, J., Ballus, C. A., Silva, L. P. da,  
581 Lozano-Sánchez, J., & Emanuelli, T. (2021). Micronization increases the  
582 bioaccessibility of polyphenols from granulometrically separated olive pomace  
583 fractions. *Food Chemistry*, 344, 128689.  
584 <https://doi.org/10.1016/j.foodchem.2020.128689>

585 Speroni, C. S., Stiebe, J., Guerra, D. R., Bender, A. B. B., Ballus, C. A., dos Santos, D.  
586 R., Morisso, F. D. P., da Silva, L. P., & Emanuelli, T. (2019). Micronization and  
587 granulometric fractionation improve polyphenol content and antioxidant capacity of  
588 olive pomace. *Industrial Crops and Products*, 137, 347–355.  
589 <https://doi.org/10.1016/j.indcrop.2019.05.005>

590 Tejada-Ortigoza, V., Garcia-Amezquita, L. E., Campanella, O. H., Hamaker, B. R., &  
591 Welti-Chanes, J. (2022). Extrusion effect on *in vitro* fecal fermentation of fruit peels  
592 used as dietary fiber sources. *LWT*, 153, 112569.  
593 <https://doi.org/10.1016/j.lwt.2021.112569>

594 Zhao, G., Zhang, R., Dong, L., Huang, F., Tang, X., Wei, Z., & Zhang, M. (2018).  
595 Particle size of insoluble dietary fiber from rice bran affects its phenolic profile,  
596 bioaccessibility and functional properties. *LWT*, 87, 450-456.  
597 <https://doi.org/10.1016/j.lwt.2017.09.016>



598

599 **Legends**

600 **Figure 1. Scheme of *in vitro* gastrointestinal digestion (oral, gastric, and intestinal**  
601 **phase) of OP samples, followed by *in vitro* colonic fermentation with fresh human**  
602 **feces.** OP: olive pomace; IN: fraction that remains inside the dialysis tube and  
603 corresponds to the digesta that will reach the colon; OUT: fraction that crosses the dialysis  
604 membrane and represents the bioaccessible fraction; NF: IN from non-fractionated OP;  
605 GF: IN from granulometrically fractionated OP; GFM: IN from granulometrically  
606 fractionated and micronized OP; Control 1: IN samples incubated with nutrient base  
607 medium, without feces; Control 2: fermentation with feces but without IN samples.

608

609 **Figure 2. Changes in phenolic alcohols and related compounds during the colonic**  
610 **fermentation of IN-OP samples.** The samples of NF, GF and GFM that remained inside  
611 the dialysis membrane (IN) after intestinal digestion, which correspond to the digesta that  
612 will reach the colon, were used for the colonic fermentation assay. Data are presented as  
613 mean  $\pm$  SEM (n = 5). \*Different from NF at the same time point ( $p < 0.05$ ). #Different  
614 from GF at the same time point ( $p < 0.05$ ). NF: non-fractionated OP; GF: granulometrically  
615 fractionated OP; GFM: granulometrically fractionated and micronized OP.

616

617 **Figure 3. Proposed biotransformation pathways for secoiridoids and phenolic**  
618 **alcohols from olive pomace during colonic fermentation.**

619

620 **Figure 4. Changes in secoiridoids during the colonic fermentation of IN-OP samples.**  
621 The samples of NF, GF and GFM that remained inside the dialysis membrane (IN) after  
622 intestinal digestion, which correspond to the digesta that will reach the colon, were used

623 for the colonic fermentation assay. Data are presented as mean  $\pm$  SEM (n = 5). \*Different  
624 from NF at the same time point ( $p < 0.05$ ). #Different from GF at the same time point  
625 ( $p < 0.05$ ). NF: non-fractionated OP; GF: granulometrically fractionated OP; GFM:  
626 granulometrically fractionated and micronized OP.

627

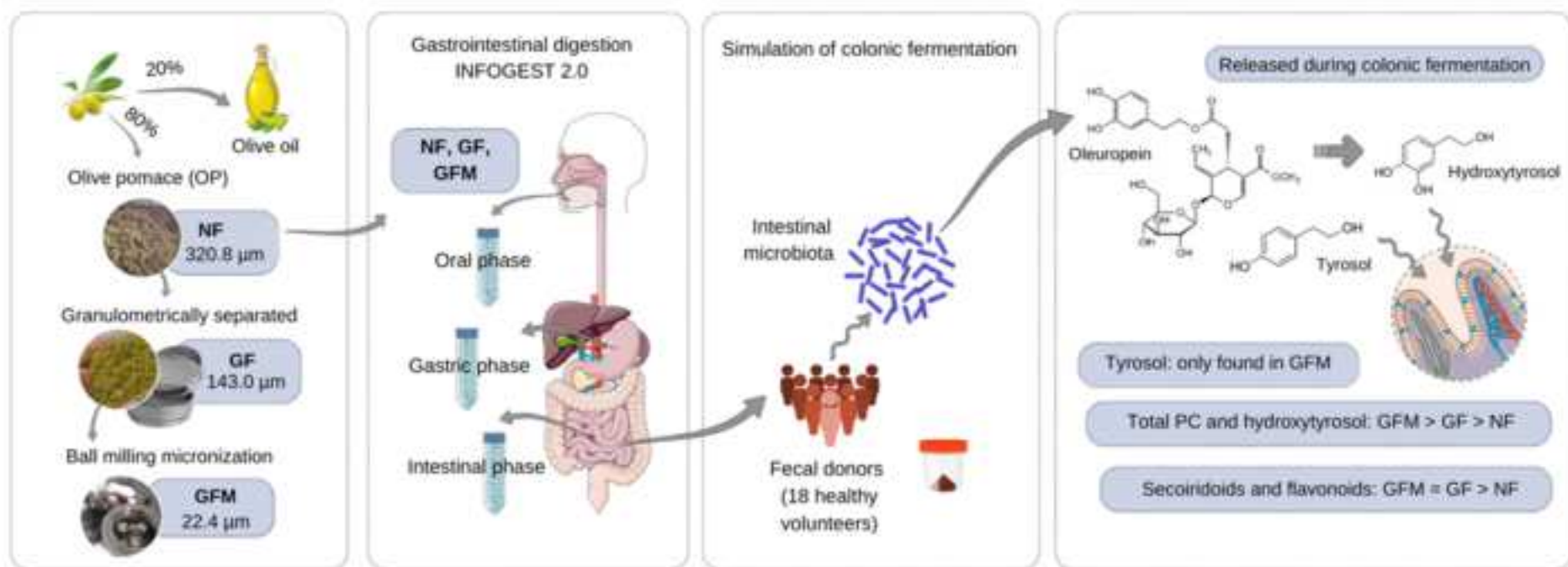
628 **Figure 5. Changes in flavonoids during the colonic fermentation of IN-OP samples.**

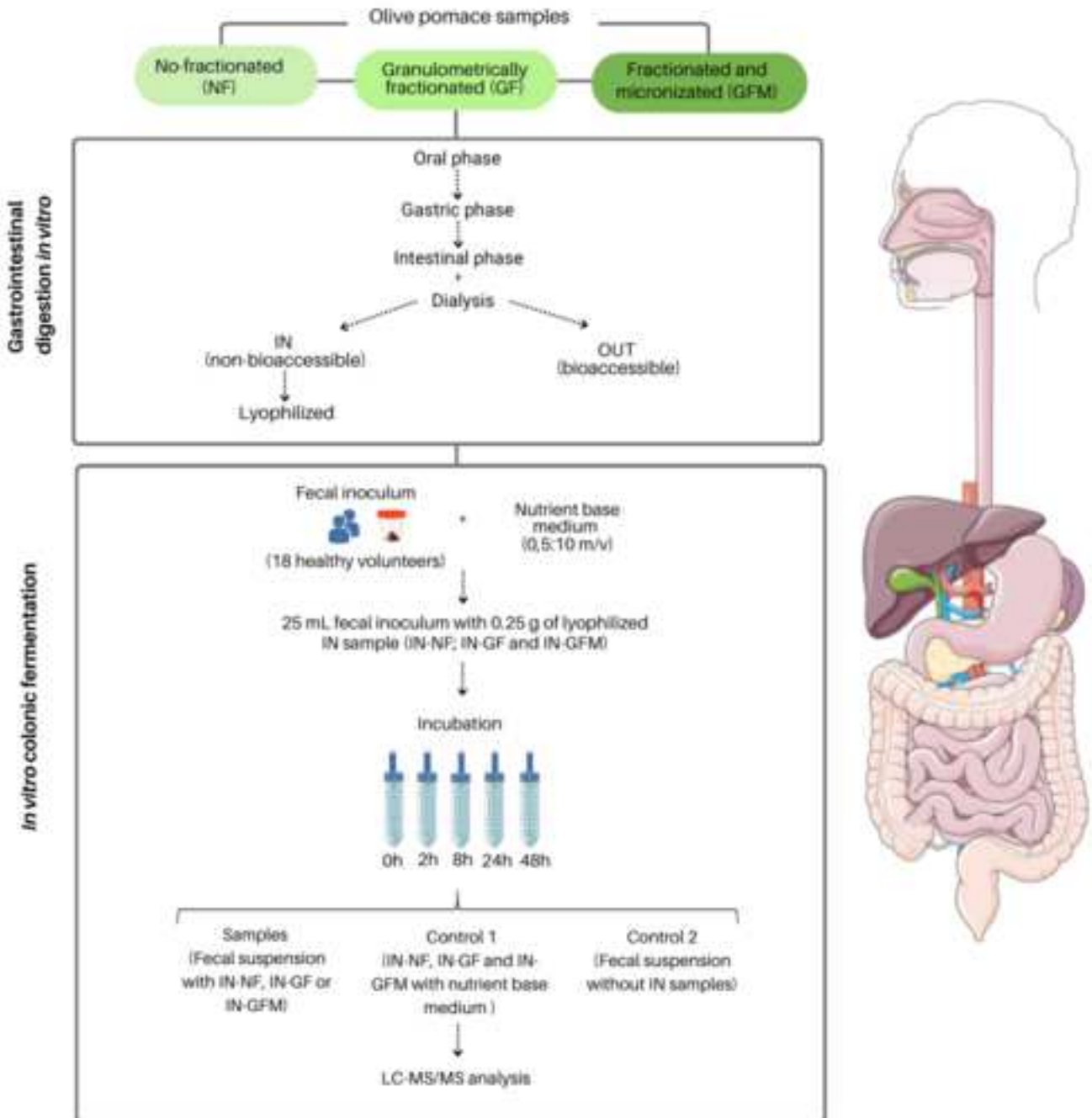
629 The samples of NF, GF and GFM that remained inside the dialysis membrane (IN) after  
630 intestinal digestion, which correspond to the digesta that will reach the colon, were used  
631 for the colonic fermentation assay. Data are presented as mean  $\pm$  SEM (n = 5). \*Different  
632 from NF at the same time point ( $p < 0.05$ ). #Different from GF at the same time point  
633 ( $p < 0.05$ ). NF: non-fractionated OP; GF: granulometrically fractionated OP; GFM:  
634 granulometrically fractionated and micronized OP.

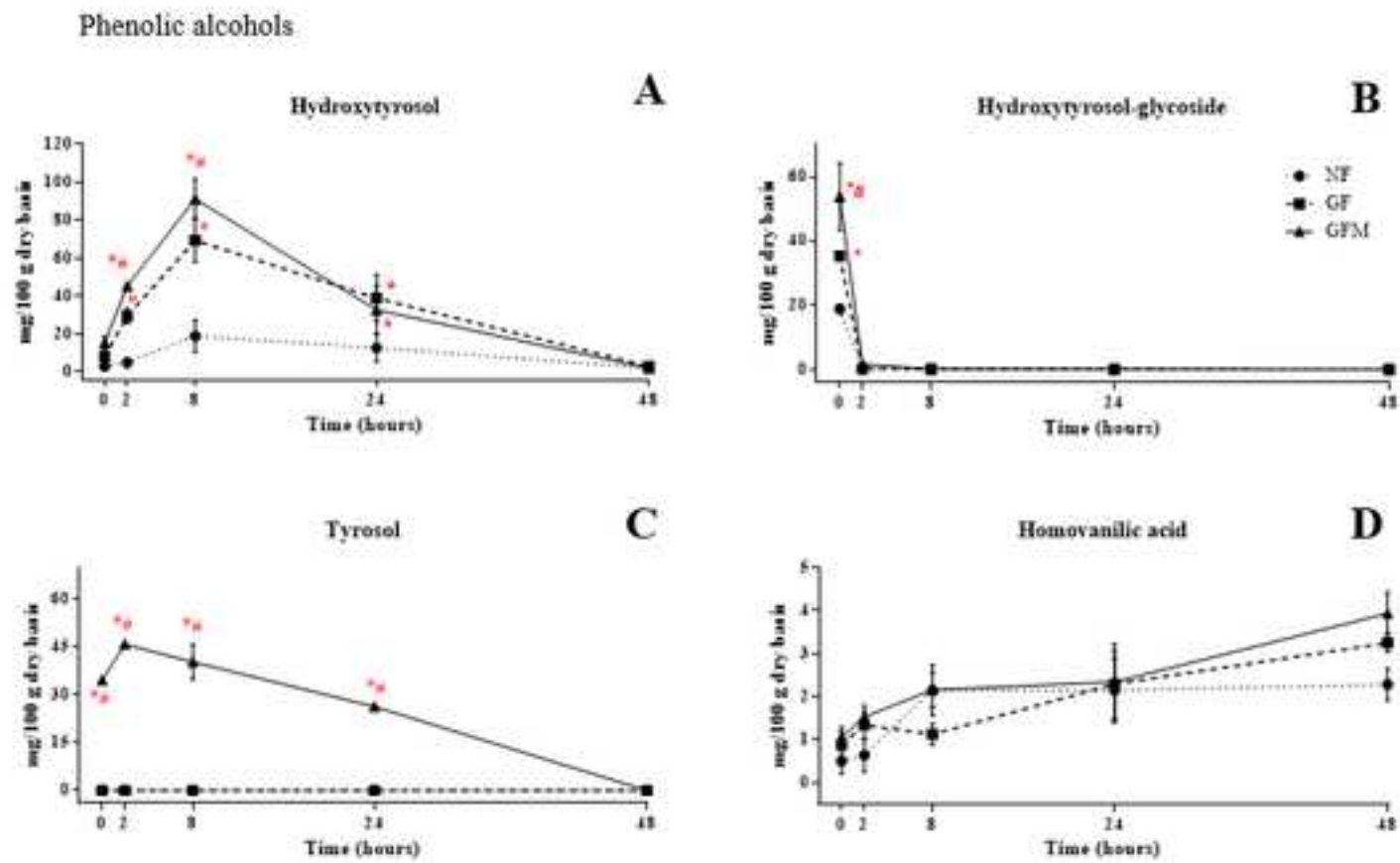
635

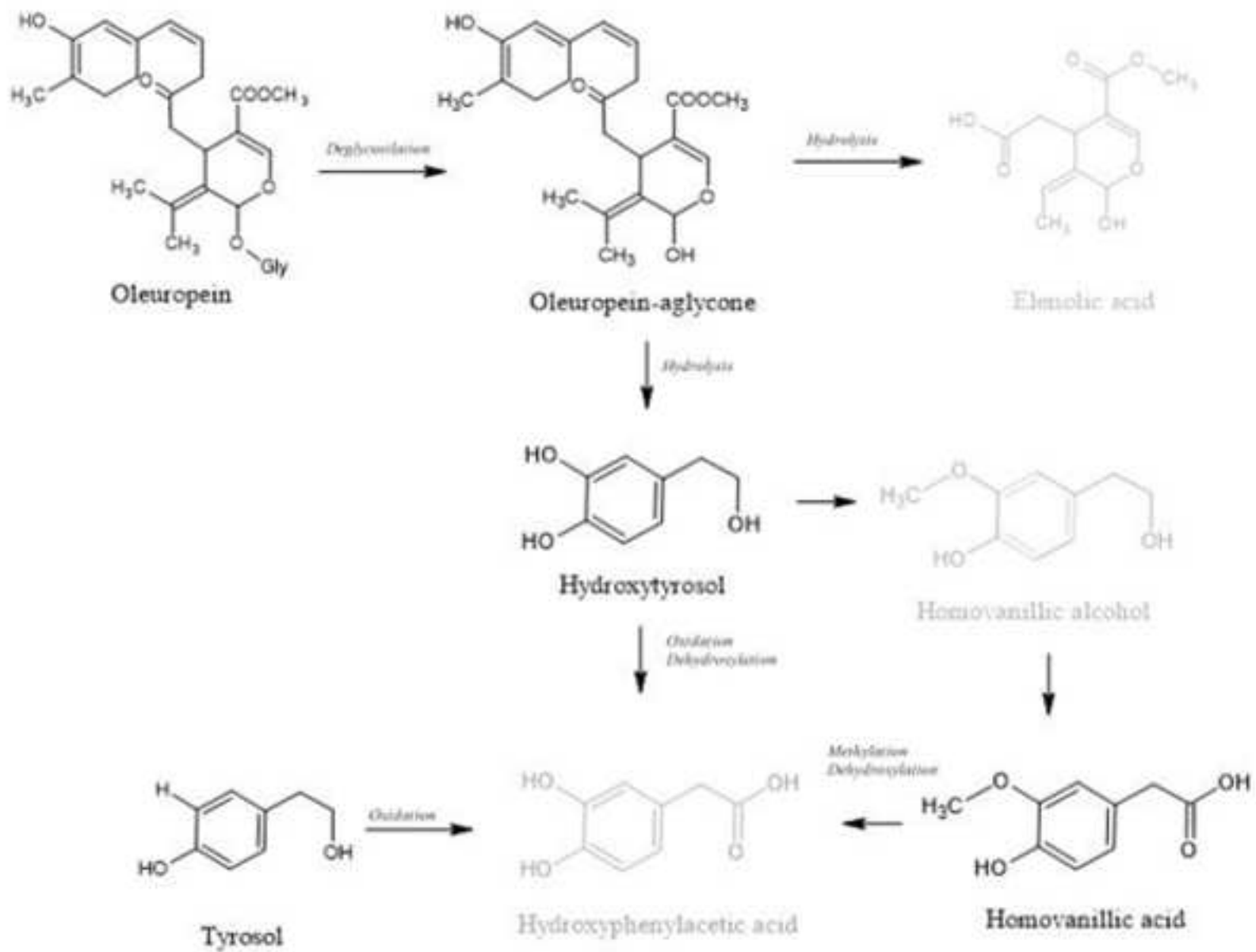
636 **Figure 6. Changes in hydroxybenzoic acids and hydroxycinnamic acids derivatives**

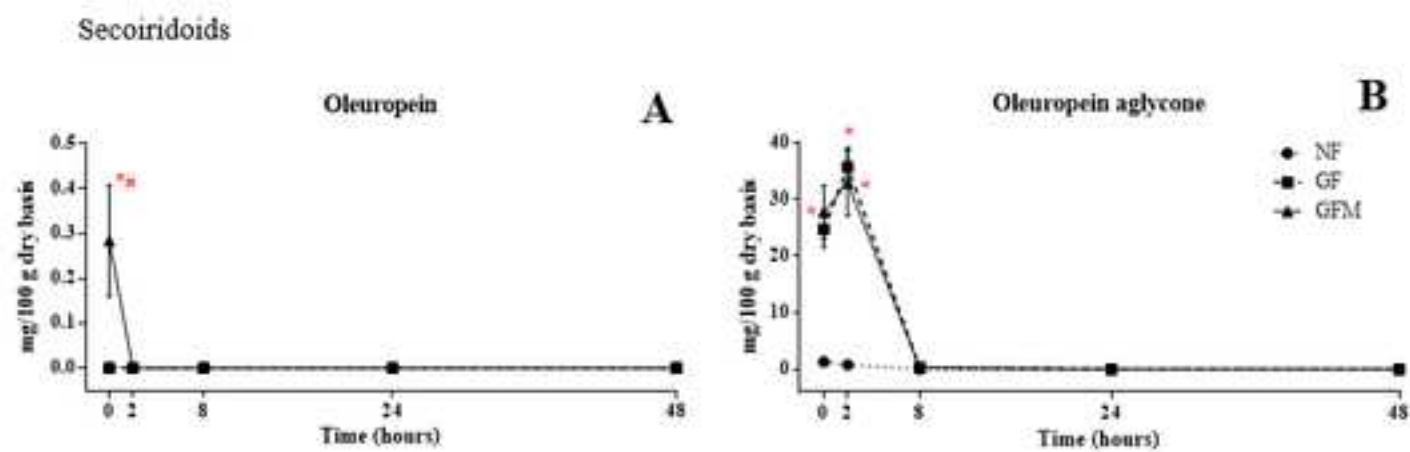
637 **during the colonic fermentation of IN-OP samples.** The samples of NF, GF and GFM  
638 that remained inside the dialysis membrane (IN) after intestinal digestion, which  
639 correspond to the digesta that will reach the colon, were used for the colonic fermentation  
640 assay. Data are presented as mean  $\pm$  SEM (n = 5). \*Different from NF at the same time  
641 point ( $p < 0.05$ ). #Different from GF at the same time point ( $p < 0.05$ ). NF: non-fractionated  
642 OP; GF: granulometrically fractionated OP; GFM: granulometrically fractionated and  
643 micronized OP.

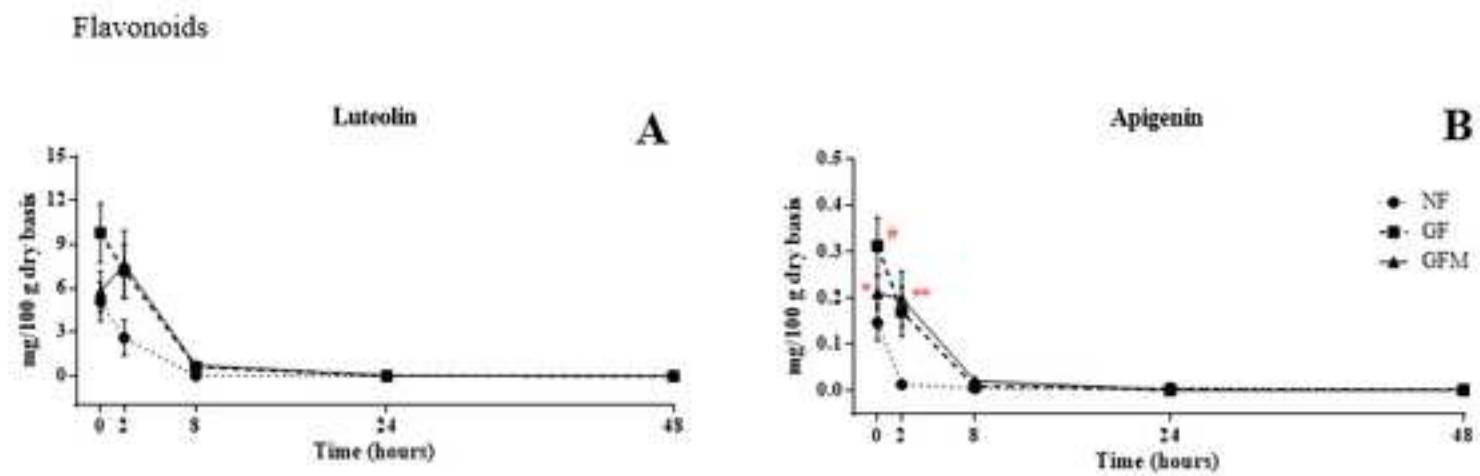




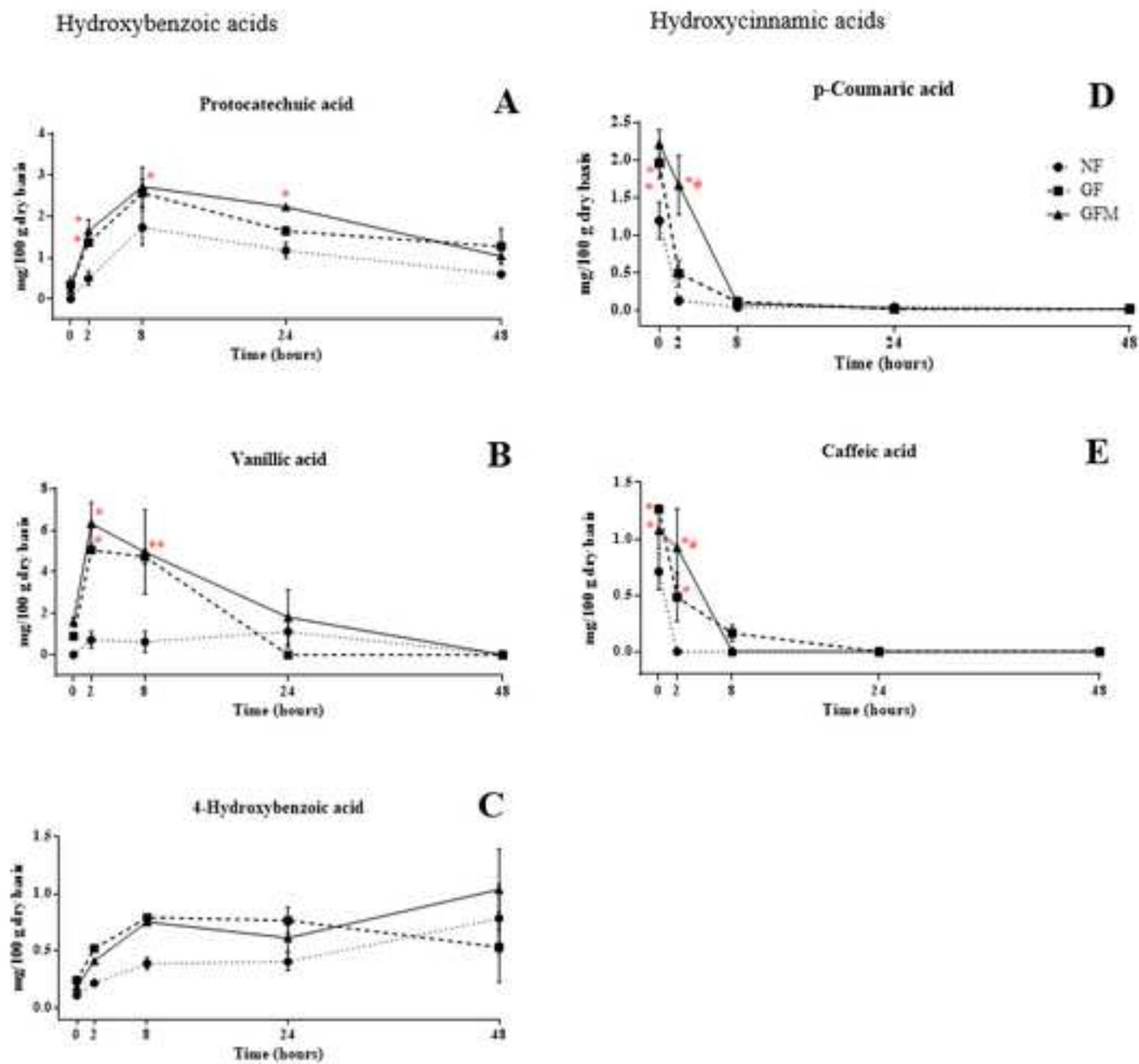












## Supplementary material

### **Effect of micronization on olive pomace biotransformation in the static model of colonic fermentation**

Camila Sant'Anna Monteiro <sup>a,b</sup>, Paula Colpo Bortolazzo <sup>b</sup>, Camila Araujo Amorim Bonini <sup>b</sup>, Luana Tamires Dluzniewski <sup>b</sup>, Dariane Trivisiol da Silva <sup>b</sup>, Julia Baranzelli <sup>a,b</sup>, Franciele Aline Smaniotto <sup>a,b</sup>, Cristiano Augusto Ballus <sup>a</sup>, Jesús Lozano-Sánchez <sup>c</sup>, Sabrina Somacal <sup>a,b</sup>, Tatiana Emanuelli <sup>a,b</sup>

Table S1. Proximate composition (g 100 g<sup>-1</sup> dry mass, except for moisture) of samples of olive pomace.

	<b>NF</b>	<b>GF</b>	<b>GFM</b>
<b>Moisture (%)</b>	9.12±0.09 a	9.29±0.08 a	8.24±0.01 b
<b>Fat</b>	4.17±0.04 b	6.94±0.02 a	7.32±0.60 a
<b>Ash</b>	2.69±0.39 b	4.37±0.20 a	4.38±0.09 a
<b>Protein</b>	0.04±0.002 b	0.09±0.000 a	0.09±0.002 a
<b>Total dietary fiber</b>	68.08±1.54 a	52.74±0.85 b	44.25±0.98 c
<b>Insoluble dietary fiber</b>	65.76±4.39 a	49.44±2.51 b	37.62±0.70 c
<b>Soluble dietary fiber</b>	2.32±2.85 b	3.30±1.66 b	6.63±0.28 a

Data are presented as mean ± SD (n = 3). Lower case letters indicate differences among samples. **NF**= non-fractionated OP; **GF**= granulometrically fractionated OP; **GFM**= granulometrically fractionated and micronized OP.

Table S2. Validation data for the analysis of phenolic compounds by LC-MS/MS analysis.

Phenolic compound	$m/z$ [M-H] <sup>-</sup>	T	CE (eV)	RT (min)	Linear range (mg L <sup>-1</sup> )	Regression equation	R <sup>2</sup>	LoD (mg L <sup>-1</sup> )	LoQ (mg L <sup>-1</sup> )	Repeatability intra-day precision CV (%)						Intermediate (inter-day) precision CV (%)	
										Low level (n=10)		Medium level (n=10)		High level (n=10)		CV (%) (n=10)	
										RT (min)	Peak area	RT (min)	Peak area	RT (min)	Peak area	RT (min)	Peak area
Pro	153	109.05	15	9.01	0.018 - 2.30	y = 2E+07x + 447958	0.9971	0.6	1.8	0.44	5.13	0.20	0.91	0.32	0.81	0.18	1.90
HT	153	123.15; 95.00	16	9.35	0.019 - 2.30	y = 9E+06x + 60531	0.9987	0.0006	0.0019	0.51	7.04	0.25	0.97	0.29	0.95	0.19	1.90
HT-gly	315	153; 123	16; 20	9.36	7.80 - 3.40	y = 6E+06x + 5E+06	0.9982	0.0006	0.0019								
4-HBA	137.2	93.1	15	11.41	0.018 - 2.30	y = 3E+07x + 136172	0.9972	0.0006	0.0018	0.25	4.17	0.12	0.86	0.20	0.64	0.12	1.33
Tyr	137.2	106; 119.1	19	11.63	3.50 - 40	y = 7566.8x - 4864.8	0.9981	1.1607	3.5172	0.33	4.86	0.22	0.87	0.25	0.95	0.18	3.21
Van	167.15	152;108.1	16; 17	13.25	0.0035 - 2.30	y = 4E+06x + 561288	0.9772	0.0012	0.0035	0.27	3.57	0.09	0.80	0.16	1.08	0.12	2.80
Caf	179.2	135.05; 134.2	16; 24	13.37	0.0012 - 2.30	y = 4E+07x + 590172	0.9991	0.0004	0.0012	0.23	3.01	0.10	0.94	0.15	1.13	0.12	5.39
HVan	181.1	137.2; 122.1	11; 16	14.23	0.0032 - 2.30	y = 2E+06x + 75852	0.9972	0.0010	0.0032	0.32	5.84	0.07	0.74	0.14	1.26	0.09	3.11
Ole-aglyc	377	197; 153	22; 16	15	0.001 - 4.40	y = 2E+07x + 664497	0.9997	0.0004	0.0013								
p-Cou	163.2	119.1	15	17.15	0.0004 - 5.0	y = 4E+07x + 4E+06	0.9984	0.0001	0.0004	0.21	1.34	0.18	0.78	0.18	1.04	0.09	2.06
Ole	539.2	377.2; 307.15	22; 16; 21	24.86	0.001 - 8.90	y = 2E+07x + 1E+06	0.9993	0.0004	0.0013	0.16	3.24	0.09	0.89	0.05	1.45	0.06	6.32
Lut	285	133; 151.05	33; 26	27.36	0.0003 - 2.30	y = 3E+07x + 1E+06	0.9986	0.0001	0.0003	0.13	2.42	0.09	1.41	0.11	1.63	0.07	7.00
Api	269	117.1; 151	35; 25	31.53	0.0003 - 2.30	y = 6E+07x + 2E+06	0.9982	0.0001	0.0003	0.11	0.49	0.08	0.90	0.16	1.29	0.08	6.07

T=transition; RT= retention time; CV= coefficient of variation; CE=collision energy Low level= LOQ of each compound; Medium level= 2.77 ppm for all compounds; High level=5 ppm for all compounds. Pro=protocatechuic acid; HT=3-Hydroxytyrosol; HT-gly=3-Hydroxytyrosol-glycoside; 4-HBA= 4-hydroxybenzoic acid; Tyr=tyrosol; Chlo=chlorogenic acid; Van=vanillic acid; Ole-agly=oleuropein aglycone; PhLac=3-Phenyllactic; Caf=caffeic acid; HVan=Homovanillic acid; p-Cou= p-coumaric acid; Verb=verbascoside; Ole=oleuropein; Lut=luteolin; Api=apigenin

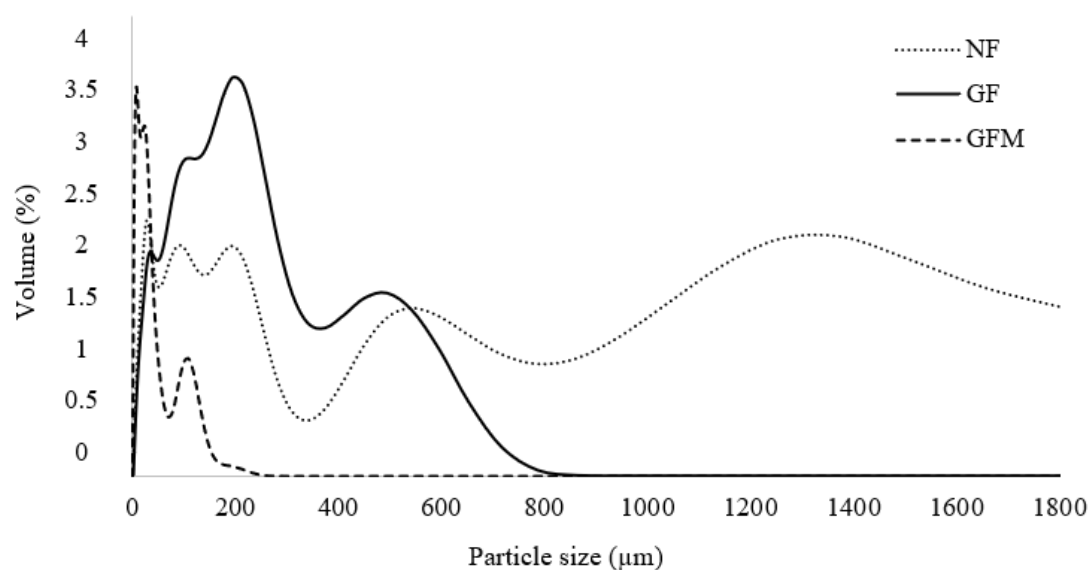


Figure S1. Particle size distribution of OP samples. NF= non-fractionated OP; GF= granulometrically fractionated OP; GFM= granulometrically fractionated and micronized OP. Results were obtained in triplicate.

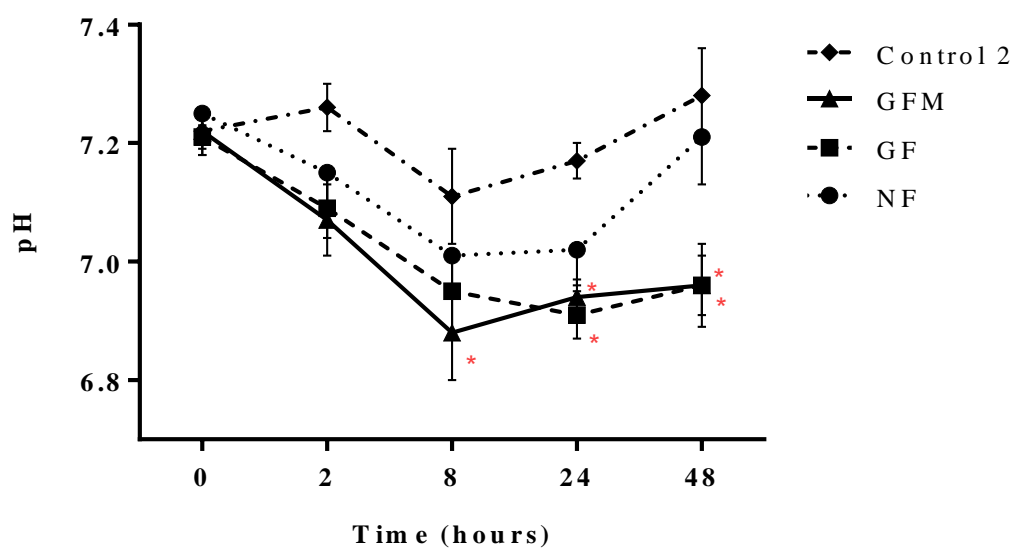


Figure S2. Changes in pH values during the colonic fermentation of IN-OP samples. The samples of NF, GF and GFM that remained inside the dialysis membrane (IN) after intestinal digestion, which correspond to the digesta that will reach the colon, were used for the colonic fermentation assay. OP: olive pomace. Control 2= fermentation with feces but without IN-OP; NF= non-fractionated OP; GF= granulometrically fractionated OP; GFM= granulometrically fractionated and micronized OP. Data are presented as mean  $\pm$  SEM (n = 5). \*Different from Control 2 at the same time point ( $p < 0.05$ ).

Table S3. Quantification of phenolic compounds during the colonic fermentation of IN-OP samples.

<i>Time</i>	0 h			2 h			8 h			24 h			48 h		
<i>Samples</i>	NF	GF	GFM	NF	GF	GFM	NF	GF	GFM	NF	GF	GFM	NF	GF	GFM
<i>Phenolic Alcohols</i>															
HT	3.0±0.18	8.1±0.94	15.21± 2.0	5.1±1.42 c	29.5±2.30 b	45.4±1.34 a	19.0±4.8 c	69.5±6.6 b	91.3±6.1 a	12.8±4.2 b	39.0±7.0 a	32.9±7.3 a	2.0±0.7	2.9±0.6	2.0±0.1
HT-gly	18.8±1.4 c	35.3±0.9 b	53.7±10.4 a	0.03±0.0	0.1±0.0	1.5±1.1	0.2±0.1	0.04±0.01	0.14±0.03	0.018±0. 01	0.05±0.04	0.01±0.0	nd	nd	nd
Tyr	nd b	nd b	34.6±1.2 a	nd b	nd b	46.2±0.8 a	nd b	nd b	40.3±5.5 b	nd b	nd	26.3±1.2	nd	nd	nd
<i>Secoiridoids</i>															
Ole	nd b	nd b	0.3±0.12 a	nd	nd	nd	nd	nd	nd	nd	nd	nd	nd	nd	nd
Ole-agly	1.3±0.3 b	24.7±3.1 9 a	27.8±4.7 a	0.8±0.3 b	35.7±3.4 a	32.9±5.8 a	nd	0.3±0.05	0.32±0.26	nd	nd	nd	nd	nd	nd
<i>Hydroxycinnamic acids</i>															
Pro	nd	0.3±0.2	0.22±0.04	0.5±0.2 b	1.4±0.08 a	1.6±0.3 a	1.8±0.4 b	2.5±0.3 a	2.8±0.4 a	1.2±0.2 b	1.6±0.1 ab	2.2±0.05 a	0.6±0.05	1.28±0. 4	1.0±0.2
Van	nd	0.9±0.08	1.6±0.22	1.2±0.5 b	5.0±0.0 a	6.3±1.0 a	1.0±0.8 b	4.8±0.3 a	4.9±2.0 a	nd	nd	4.5±2.2	nd	nd	nd
4-HBA	0.1±0.02	0.2±0.02	0.2±0.02	0.216±0.02	0.5±0.03	0.4±0.01	0.4±0.05	0.8±0.02	0.8±0.02	0.4±0.08	0.7±0.1	0.6±0.1	0.8±0.3	0.5±0.3	1.0±0.3
<i>Hydroxybenzoic acids</i>															
<i>p</i> -Cou	1.2±0.2 b	2.0±0.2 a	2.2±0.19 a	0.1±0.05 b	0.5±0.17 b	1.7±0.4 a	0.05±0.01	0.1±0.06	0.1±0.03	0.05±0.0 1	0.02±0.01	0.03±0.01	0.02±0.0	0.02±0	0.02±0.0
Caf	0.7±0.16 b	1.2±0.03 a	1.0±0.01 a	nd c	0.5±0.2 b	0.9±0.3 a	nd	0.2±0.07	nd	nd	nd	nd	nd	nd	nd
<i>Flavonoids</i>															

Lut	5.0±1.3	9.7±2.0	5.8±1.4	2.6±1.2	7.2±1.8	7.6±2.3	nd	0.6±0.2	0.7±0.1	nd	nd	nd	nd	nd	nd
Api	0.1±0.04 b	0.3±0.06 a	0.2±0.03 b	0.01±0.01 b	0.2±0.05 a	0.2±0.06 a	nd	nd	nd	nd	nd	nd	nd	nd	nd
<i>Other compounds</i>															
Verb	0.4±0.1	1.9±0.2	3.0±1.3	0.2±0.2	2.0±1.2	2.1±1.2	nd	nd	nd	nd	nd	nd	nd	nd	nd
HVan	0.5±0.3	0.9±0.3	1.0±0.24	0.6±0.4	1.3±0.3	1.5±0.3	2.1±0.6	1.1±0.2	2.1±0.4	2.1±0.7	2.3±0.8	2.4±0.9	2.3±0.4	3.3±0.2	4.0±0.5
Total	31.1	85.5	146.7	11.4	83.8	148.2	24.5	79.2	143.5	16.5	43.7	68.9	5.7	7.0	8.0

The samples of NF, GF and GFM that remained inside the dialysis membrane (IN) after intestinal digestion, which correspond to the digesta that will reach the colon, were used for the colonic fermentation assay. OP: olive pomace. NF= non-fractionated OP; GF= granulometrically fractionated OP; GFM= granulometrically fractionated and micronized OP. Data are presented as mean ± SEM (n = 5). ND = not detected. Lower case letters indicate differences among samples at the same fermentation time ( $p < 0.05$ ). Pro=protocatechuic acid; HT=3-Hydroxytyrosol; HT-gly=3-Hydroxytyrosol-glycoside; 4-HBA= 4-hydroxybenzoic acid; Tyr=tyrosol; Van=vanillic acid; Ole-agly=oleuropein aglycone; Caf=caffeic acid; HVan=Homovanillic acid; p-Cou= *p*-coumaric acid; Verb=verbascoside; Ole=oleuropein; Lut=luteolin; Api=apigenin.

**Declaration of interests**

The authors declare that they have no known competing financial interests or personal relationships that could have appeared to influence the work reported in this paper.

The authors declare the following financial interests/personal relationships which may be considered as potential competing interests:



**CRedit authorship contribution statement**

**Camila Sant'Anna Monteiro:** Investigation, Methodology, Data curation, Conceptualization, Writing - original draft, Writing - review & editing, Visualization.

**Paula Colpo Bortolazzo:** Investigation, Methodology, Visualization, Data acuration.

**Camila Araujo Amorim Bonini:** Investigation, Visualization, Methodology. **Luana**

**Tamires Dluzniewski:** Investigation, Visualization. **Dariane Trivisiol da Silva:**

Investigation, Methodology. **Julia Baranzelli:** Formal analysis, Visualization,

Methodology. **Franciele Aline Smaniotto:** Investigation, Visualization, Methodology.

**Cristiano Augusto Ballus:** Writing - review & editing, Methodology. **Jesús Lozano-**

**Sánchez:** Writing - review & editing, Formal analysis. **Sabrina Somacal:** Investigation,

Writing - review & editing, Data curation, Visualization. **Tatiana Emanuelli:**

Conceptualization, Resources, Supervision, Writing – original draft, Writing - review & editing, Funding acquisition, Project administration.